Absorption and Magnetic-Circular-Dichroism Spectra of Octahedral Ce^{3+} in Cs_2NaYCl_6

R. W. Schwartz* and P. N. Schatz
Department of Chemistry, University of Virginia, Charlottesville, Virginia 22901
(Received 14 March 1973)

The $4f^1 \rightarrow 5d^1$ transitions of Ce^{3+}, $E_u''(^2F_{5/2}) \rightarrow U_g'(^2T_{2g})$ and $E_u''(^2F_{5/2}) \rightarrow E_g''(^2T_{2g})$ have been studied at precisely octahedral sites using absorption and magnetic-circular-dichroism (MCD) techniques at liquid-helium temperature. The no-phonon lines of the two transitions are located at 28 196 and 29 435 cm^{-1}, respectively. Considerable vibronic structure is resolved in both bands characterized by long progressions in $\nu_1(a_{1g})$ of the $CeCl_6^{3-}$ moiety with low-energy lattice progressions superimposed. The U_g' and E_g'' excited states show a spin-orbit splitting of ~ 1240 cm^{-1} versus a predicted free-ion value of $3\zeta_d/2 \approx 1500$ cm^{-1}. The MCD spectrum strongly supports the proposed assignments. There are no indications of a significant Jahn-Teller effect in the $U_g'(^2T_{2g})$ excited state. Since no further Ce^{3+} absorption is detected out to 50 000 cm^{-1}, $\Delta(\equiv 10Dq) \geq 20\,000$ cm^{-1} in the excited state.

I. INTRODUCTION

The magnetic-circular-dichroism (MCD) technique has recently been employed with considerable success to elucidate the low-temperature high-resolution optical spectra of several octahedral transition-metal hexahalides doped into cubic hosts.[1-4] This technique is applied here to study, at high resolution and in an octahedral environment, the simplest $f \rightarrow d$ transition arising in the lanthanides. Although many spectroscopic studies of lanthanides have been reported in cubal (eight-coordinate) environments,[5] little or no work appears to have been done on these ions at precisely octahedral (six-coordinate) crystal sites.[6] This is now possible for lanthanides (and other ions) in the 3+ oxidation state following the work of Morss *et al.*,[7] who recently reported that the trivalent ion M in the cubic crystals Cs_2NaMCl_6 is six-coordinate at a site of O_h symmetry (with M any one of a variety of ions). These workers suggested that such crystals would be useful for studying various properties of trivalent ions, though only one study seems to have appeared so far—involving paramagnetic-susceptibility measurements on the pure material $Cs_2NaYbCl_6$.[8] Our report describes the first of a series of optical studies using the transparent (to at least 2000 Å) diamagnetic host Cs_2NaYCl_6, which accepts as dopants a variety of trivalent rare-earth and first-row transition-metal ions, as well as several tetravalent third-row ions.

Ce^{3+} is of interest for several reasons. Since the ground-state configuration is f^1, it is possible to study the simplest $f \rightarrow d$ transition in an environment which an EPR study shows to be octahedral and which produces a spectrum exhibiting considerable vibronic fine structure. In addition, the excited d^1 configuration gives rise to two Jahn-Teller susceptible U' states. In previous work on $CaF_2:Ce^{3+}$, the observation of a dynamic Jahn-Teller effect was reported for the $U_g'(^2E_g)$ state.[9] Subsequent analysis,[10] however, very strongly indicated that the reported effects were attributable to Ce^{3+} ions at tetragonally distorted (charge-compensated) sites which indeed precluded the possibility of a Jahn-Teller effect. In the present work, there is no charge-compensation problem and evidence for Jahn-Teller effects can be sought in an ion whose site symmetry is well characterized. Since the environment is octahedral rather than cubal (as for $CaF_2:Ce^{3+}$), the crystal-field splitting has opposite sign and the $^2T_{2g}$ term is observed rather than the ^2E_g state discussed in Refs. 9 and 10. $^2T_{2g}$, however, is split under the large spin-orbit coupling, into a lower energy U_g' and a higher-energy E_g'' state, the former of which is itself Jahn-Teller susceptible.

II. EXPERIMENTAL

Cs_2NaYCl_6 was prepared by method E of Morss *et al.*[7]; i.e., evaporating an HCl solution of the requisite anhydrous chlorides to dryness. The material thus obtained had an x-ray-diffraction powder pattern similar to those given[7] for some isomorphous salts. Neither CsCl nor NaCl, the two most likely impurities, were detected in significant amounts. The powder pattern could be indexed well with the previously reported lattice constant of 10.73 Å.[7] All material prepared in this way contained small amounts of impurities. Fe^{3+} from HCl is possibly one; another has been shown to be present in 99.9% YCl_3 but has not yet been identified. All impurity absorptions are observed in the spectrum of an undoped crystal and in no way interfere with the Ce^{3+} spectrum reported here. The impurity bands, in general, are broad and featureless and decrease in intensity as the crystal is cooled showing that they correspond to forbidden transitions, in contrast to the allowed Ce^{3+} transitions which will be discussed.

Single crystals were grown in vacuum-sealed quartz ampoules by the Bridgeman technique. The

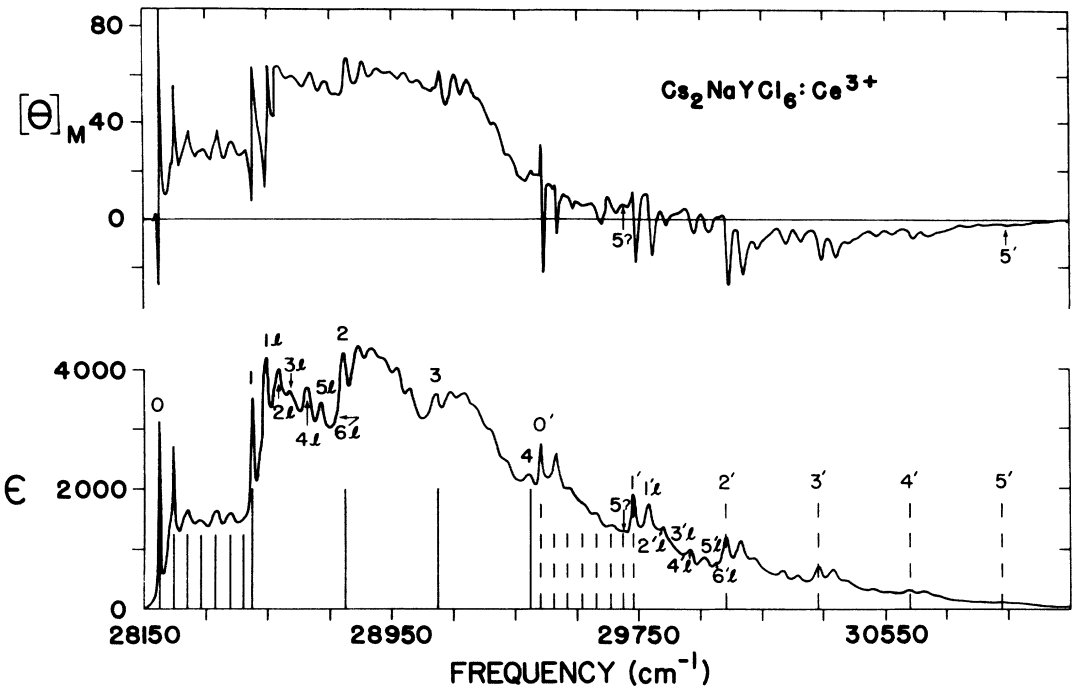

FIG. 1. Absorption and MCD spectrum of $Cs_2NaYCl_6:Ce^{3+}$ at about 6 °K. $[\theta]_M$ is the MCD in molar ellipticity units (defined as in natural optical activity) per gauss in the direction of the light beam. $[\theta]_M = 3.30\times10^3(\epsilon_L - \epsilon_R)/H$. ϵ is the molar extinction coefficient (optical density divided by the product of concentration in mole liter^{-1} and sample thickness in cm). The Ce^{3+} concentration is approximately $5.5\times10^{-3}M$, and rough *absolute* values of ϵ and $[\theta]_M$ are reported. The bar spectrum shows the calculated positions of vibronic lines for the U_g' state (solid bars) and E_g'' state (dashed bars) assuming $\nu_1(a_{1g}) = 300$ cm^{-1} (large vertical bars) and ν(lattice) = 45 cm^{-1} (small vertical bars). For clarity, the progressions $1l$-$6l$ and $1'l$-$6'l$ are labeled at their *first repeat* in $\nu_1(a_{1g}) \approx 300$ cm^{-1} (see Table II for detailed assignments).

dropping rate was about 3 in. per day, and the maximum temperature was between 850 and 900 °C. The small quantity of Ce^{3+} dopant was added as the sulfate salt. It seemed unlikely that the sulfate would remain coordinated to the Ce^{3+} in the resulting doped crystal since the material was in a molten state for several days. This is confirmed by EPR measurements[11] which show that the Ce^{3+} sites are precisely octahedral (see below).

MCD and absorption spectra were measured using a Durrum-Jasco J-10B CD-UV spectrophotometer interfaced with a Spex 1400-II $\frac{3}{4}$-m double-grating monochromator. Spectral slit widths between 2 and 10 cm^{-1} were used. Complete resolution was not always achieved, but the structure of all essential features was ascertained. The absorption spectrum was also recorded out to 50 000 cm^{-1} on a Cary 14 spectrophotometer, and there are no indications of additional features that can be attributed to Ce^{3+}.

A rough (± 50%) determination of Ce-atom concentration was made using high-resolution spark-source mass-spectrometric techniques. It was found that the ratio of Ce to Cs atoms in the doped crystal was $(5.6\pm2.8)\times10^{-4}$. From the known crystal structure of the host, one calculates a Ce^{3+} concentration of 5.48×10^{-3} mole liter^{-1}. Measuring the crystal thickness (± 5%) thus permits rough *absolute* values of ϵ and $[\theta]_M$ to be reported (Figs. 1 and 2). The most significant theoretical quantities are ratios of an MCD and absorption parameter (e.g., A/D or C/D) which are independent of concentration uncertainties. *Relative* spectral amplitudes in the absorption and MCD spectra should be good, respectively, to ± 15% and ± 25%.

All spectra shown were recorded using the Spex monochromator which was calibrated against known wavelengths of a mercury arc lamp. The frequencies of sharp peaks should be good to about ± 5 cm^{-1}.

III. RESULTS AND DISCUSSION

A. Assignment of Electronic Transitions

Figure 1 shows the MCD and absorption spectrum of $Cs_2NaYCl_6:Ce^{3+}$ recorded at (6.0 ± 0.5) °K. The integrated absorption intensity remains approximately constant as the temperature is lowered to 6 °K, and this coupled with observed ϵ values greater than 10^3 conclusively demonstrates the allowed nature of the transitions. (At room temperature, the entire absorption region consists of a single smooth band.) It seems well established

that $f \rightarrow d$ transitions are expected for Ce^{3+} in this energy range,[9,10,12] and the spectra are interpreted on this basis. Since the ground state is degenerate, the MCD spectrum should be dominated by C terms (which vary as T^{-1}).[13] This is strongly suggested by the very large $[\theta]_M$ values observed and has been explicitly confirmed by observing the expected T^{-1} dependence in the ~(6–20) °K range. A terms will only be observed for sharp lines since their peak-to-trough amplitude varies as the inverse second power of the linewidth.[13]

There are two electronic transitions. Measured by the no-phonon line frequencies, these are located at 28 196 (line 0) and 29 435 cm^{-1} (line 0′). The first band consists of a series of negative C terms[13] (positive MCD) with positive A terms[13] also evident for some of the lines. The second transition shows a series of positive C terms accompanied by negative A terms. There is considerable overlap of the two bands since the a_{1g} progression in the first no-phonon line (lines 1–4) extends at least through four quanta. Line 4 (Fig. 1) at ~29 400 cm^{-1} is only slightly to the red of the no-phonon line of the second transition, and there is an indication of line 5 at ~29 700 cm^{-1}. The association of line 0′ at 29 435 cm^{-1} with a new electronic transition seems especially obvious in the MCD pattern where a sharp *negative* A term appears for the first time.

The assignment of the two observed transitions can be conveniently discussed using the schematic energy-level diagram of Fig. 3. The f^1 ground state of Ce^{3+} gives rise, in the atomic case, to a ^2F term which splits into $^2F_{5/2}$ and $^2F_{7/2}$ states

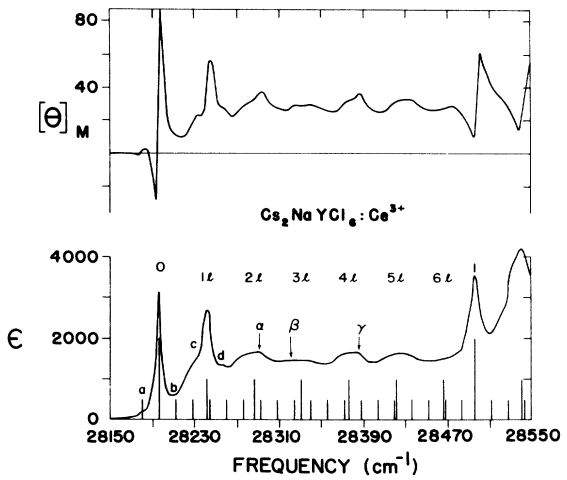

FIG. 2. Detail of the MCD and absorption spectrum from Fig. 1 showing the first set of absorptions in the U_g' excited state. The large, medium, and small vertical bars show calculated positions, respectively, of the 300-, 45- and 16-cm^{-1} progressions (see Table II for detailed assignments). Units are as in Fig. 1.

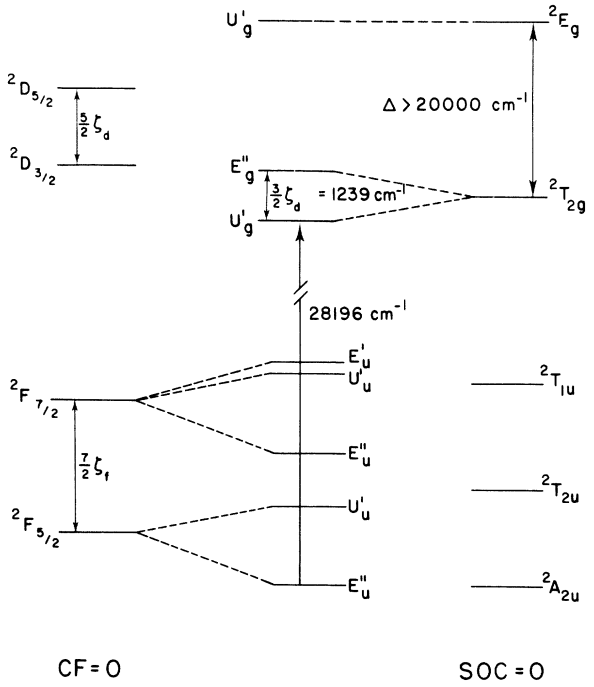

FIG. 3. Schematic energy-level diagram for six-coordinated Ce^{3+} in O_h symmetry. Dashed lines show correlations with closest limiting case. Some observed energies and calculated splittings for Ce^{3+} in Cs_2NaYCl_6 are also shown. For Ce^{3+}, the *free-ion* values are (Ref. 18) $\zeta_f = 644$ cm^{-1}, $\zeta_d = 996$ cm^{-1}.

under spin-orbit coupling. To first order, the splitting is $\frac{7}{2}\zeta_f$ with $^2F_{5/2}$ lowest. $^2F_{5/2} \rightarrow {}^2F_{7/2}$ transitions have been directly observed in the expected 2000–3000-cm^{-1} range in CeF_3 and in $LaF_3:Ce^{3+}$.[14] In the octahedral field of the six chloride ligands, the $^2F_{5/2}$ ground state will split into E'' and U' components[15] separated by an unknown amount, presumably of the order of 10^2 cm^{-1}. Simple crystal-field theory predicts that the E'' state will be lowest.[16] This is confirmed by liquid-helium EPR measurements on single crystal and powder samples which show a single isotropic resonance, with a half-width of 10 G, corresponding to a $|g|$ value of 1.266(3).[11] An isolated $E''(^2F_{5/2})$ state in octahedral symmetry would give a $|g|$ value of 1.429,[17] but this discrepancy can be readily accounted for by assuming that either ~1% or ~12% $E''(^2F_{7/2})$ is mixed into the ground state.[11] A U' ground state would not give an isotropic EPR spectrum.[17] *The isotropic behavior of the EPR resonance shows that the* Ce^{3+}*-ion ground-state site symmetry is* O_h.

In contrast to the more usual (approximately) cubal site symmetry,[5,9,10] the Ce^{3+} ions are octahedrally coordinated in the present case, and thus the crystal-field splitting has the t_{2g} orbitals *below* the e_g. In Fig. 3, the ground-state f manifold is

TABLE I. Theoretical and experimental parameters.[a]

		$\frac{A_1}{D_1}$[b]	$\frac{C_1}{D_1}$[b]	$\frac{A_2}{D_2}$[b]	$\frac{C_2}{D_2}$[b]	$\frac{C_1+C_2}{D_1+D_2}$[b]	$\frac{D_1}{D_2}$
Theory	$\kappa=1.0$ $\lvert g\rvert=1.429$[c]	0.357	−0.357	−1.714	0.714	−0.336	50
	$\kappa=0.83$[d] $\lvert g\rvert=1.429$[c]	0.499	−0.357	−1.601	0.714	−0.336	50
	$\kappa=1.0$ $\lvert g\rvert=1.266$[e]	0.316	−0.316	−1.633	0.633	−0.298	50
Experiment	integration[f]		(−)		(+)	−0.14	~10[g]
	individual lines	0.21[h]	−0.17[h]	(−)	(+)		

[a]Subscripts 1 and 2 refer, respectively, to the transitions $E_u''(^2F_{5/2}) \rightarrow U_g'(^2T_{2g})$ and $E_u''(^2F_{5/2}) \rightarrow E_g''(^2T_{2g})$. Details of the theoretical calculations are summarized in the Appendix. B-term effects (field-induced mixing) (Ref. 13) are not included since they integrate approximately to zero over both transitions. This follows when it is recognized that amplitudes comparable to the observed C terms are possible only for field-induced mixing between the two partially overlapping electronic bands, and this effect produces pairs of B terms *equal* in magnitude but *opposite* in sign.

[b]Units of Bohr magnetons.

[c]$\lvert g\rvert$ value calculated assuming the ground state is pure $E_u''(^2F_{5/2})$.

[d]A lower limit for κ obtained by taking the ratio of observed to theoretical spin-orbit splitting.

[e]$\lvert g\rvert$ value measured in EPR spectrum (Ref. 11).

[f]Integrations are over the entire spectral region of Fig. 1 and involve the relations $(C_1+C_2)/kT=-(1/33.53)\int([\theta]_M/\nu)\,d\nu$ and $D_1+D_2=9.1834\times10^{-3}\int(\epsilon/\nu)d\nu$ (Ref. 13).

[g]Very rough guess—see text.

[h]A_1 and C_1 determined by Gaussian fit of line 0. D_1 obtained by numerical integration of line 0 excluding line *a* and assuming that total area is twice area of low-energy half of line.

much more closely represented by the left-hand side of the diagram (^2F) while the excited-state d manifold is close to the right-hand side ($^2T_{2g}$, ^2E_g). This reflects the fact that spin-orbit coupling is much more important than the crystal field in the f manifold and vice versa for the d manifold. The actual states are shown in the middle of Fig. 3. The ordering within the f manifold is a plausible one selected from an octahedral $5f^1$ case (NpF_6).[16]

In contrast to the cubal case where the first strong region of absorption corresponds to a single electronic transition to $U_g'(^2E_g)$, two electronic transitions are expected in this case separated by $\sim\frac{3}{2}\zeta_d$, where $\zeta_d\approx1000$ cm^{-1} is the free-ion spin-orbit coupling constant for a Ce^{3+} $5d$ electron.[18] A splitting of the expected magnitude is indeed observed (experimental value = 1239 cm^{-1}), which corresponds to a quite reasonable reduction from the free-ion value (nephelauxetic effect).[19] The transitions are therefore assigned (from low to high energy) as $E_u''(^2F_{5/2}) \rightarrow U_g'(^2T_{2g})$ and $E_u''(^2F_{5/2}) \rightarrow E_g''(^2T_{2g})$, respectively. The MCD spectrum provides immediate support for these assignments since positive A and negative C terms are associated with the no-phonon line of the first transition and vice versa for the second, in direct accord with the theoretical calculations (Table I and Appendix) which are certainly reliable in sign. It is also possible to extract rough quantitative values of some of the parameters for comparison with theory, and the results are summarized in Table I. Only line 0 is sufficiently isolated in both absorption and MCD to permit a direct estimate of parameters for a single electronic transition. The signs are as predicted and the ratio of A/C agrees well with theory. The ratios A/D and C/D are appreciably low compared to the theoretical parameters which are probably most accurately represented by the $\kappa=1.0$, $\lvert g\rvert=1.266$ case. The integrated quantity $(C_1+C_2)/(D_1+D_2)$ is similarly low in comparison to theory. Even taking all uncertainties into account, a real discrepancy seems probable. Furthermore, though the two absorption bands are so strongly overlapped as to completely preclude an accurate determination of individual electronic dipole strengths, a rough *guess* suggests a ratio of ~10 (or even perhaps 20) in contrast to the theoretical ratio of 50 (see Appendix). It should, however, be noted that the theoretical ratio $D_1/D_2=50$ is extremely sensitive to deviations from the simple model used—for example, to the assumption that the ground state is pure $E_u''(^2F_{5/2})$. If $E_u''(^2F_{7/2})$ is

appropriately mixed into the ground state (~1% or ~12%), the experimental g value can be reproduced. However such mixings produce calculated D_1/D_2 ratios of 440 or 2.9, respectively, neither of which accords with experiment. In fact, it seems likely that D_1/D_2 is sensitive to even small amounts of mixing of metal and ligand orbitals, and detailed consideration of this possibility would probably be required to explain the experimental ratios.

It was mentioned previously (Sec. II) that no further Ce^{3+} absorption was observed out to 50 000 cm^{-1} implying that $\Delta(\equiv 10Dq) \gtrsim 20\,000$ cm^{-1}. McClure and Kiss[20] quote an unpublished value of $Dq = 2050$ cm^{-1} for Ce^{3+} in CaF_2 based on work of Struck. This is consistent with the present observation since the crystal-field splitting in cubal CaF_2 should be $\sim\frac{8}{9}\Delta$, and Δ values for Cl^- are typically ~10% less than for F^-.[12(b)]

Since there is little doubt regarding the assignment of the electronic transitions, attention will now be directed to the detailed vibronic structure.

B. Assignment of Vibronic Fine Structure

Since the two electronic transitions are allowed, the most prominent vibronic features should be a_{1g} progressions built on each of the no-phonon lines. Indeed, there is a very clear ~300-cm^{-1} progression labeled 0, 1, 2, 3, 4, 5? for the first (lower-energy) transition and 0′, 1′, 2′, 3′, 4′, 5′ for the second (higher-energy) transition which undoubtedly arises from the a_{1g} breathing mode ν_1 of the $CeCl_6^{3-}$ moiety. Such a pattern is commonly observed in hexahalide systems.[1-4] However, Fig. 1 reveals much additional structure.

The EPR results[11] previously quoted demonstrated precise O_h ground-state site symmetry at the Ce^{3+} ions. It seems likely that this is at least approximately true in the two electronic excited states discussed here. Specifically, the no-phonon line of the first band, at 28 196 cm^{-1}, is quite sharp (halfwidth ~6 cm^{-1}) and shows no obvious splitting. If the Ce^{3+} ion in this excited state resided at a site of lower symmetry, this line would be expected to split into two Kramers doublets. It seems reasonable to make a similar assumption for the second transition (starting with line 0′ at 29 435 cm^{-1}) though no splitting of this nature is possible because the excited electronic state is a Kramers doublet. Under these circumstances, only g excited-state vibrations can be seen (in the electric-dipole approximation) since the electronic transitions are $u \rightarrow g$.

The U_g' excited state is Jahn-Teller susceptible, whereas the E_g'' excited state is not. Thus, to first order, t_{2g} or e_g modes can borrow intensity from the no-phonon line in the first case but can only appear via out-of-state (Herzberg-Teller) mixing in the second. In actual fact, the vibronic structure in both bands is quite similar and, in addition to the ν_1 progression in the no-phonon lines, is characterized by approximately equally spaced (~45 cm^{-1}) series of lines ($1l - 6l$ and $1'l - 6'l$) which are repeated several times in ν_1. The low frequency indicates a lattice mode, and the basic similarity in pattern for the two electronic transitions suggests a common mechanism. It seems likely that the series $1l - 6l$ and $1'l - 6'l$ constitute progressions in a totally symmetric localized or pseudolocalized lattice mode.[21] This same effect was observed previously in $Cs_2ZrBr_6:Ir^{4+}$ (band 6),[4] and similar effects in molecular crystals have been discussed recently.[22]

There is some further structure evident within the first ν_1 quantum of the lower-energy transition, and this region is displayed in greater detail in Fig. 2. First, there is a very weak line (labeled a) ~16 cm^{-1} *to the red* of the no-phonon line. It is seen quite clearly in the MCD and has the same sign and approximate A/C ratio as the no-phonon line. About the same energy to the blue of the no-phonon line is a barely perceptible shoulder which is not well resolved either in absorption or MCD (line b). It seems likely that the ~16-cm^{-1} frequency corresponds to another lattice mode with a hot band mirrored ~16 cm^{-1} to the red of the no-phonon line. The energy is certainly low enough to permit appreciable population of the first vibrational excited state at the temperature of the experiment (~6 °K). As the temperature of the crystal is raised, the lines broaden rapidly, and no further information is obtained. There is additional structure on both shoulders of line $1l$ and on several of the higher energy lines in Fig. 2. Lines c and d line up well as members of a progression in the 16-cm^{-1} lattice mode (see bar spectrum, Fig. 2). Lines α, β, and γ are discussed below. No additional structure was resolved beyond line 1 in the first electronic transition or anywhere in the second electronic transition. A detailed assignment of most of the vibronic structure is summarized in Table II.

Finally, consideration should be given to the possibility of a Jahn-Teller effect in the lower-energy transition. The frequencies of the Jahn-Teller active "internal" modes [$\nu_2(e_g)$ and $\nu_5(t_{2g})$] of $CeCl_6^{3-}$ do not appear to have been measured, but ground-state data are available for the closely related $4f^0$ system $CeCl_6^{2-}$.[23] These frequencies should certainly not differ markedly from those of our moiety.[23] The g frequencies (in cm^{-1}) are[23] $\nu_1(a_{1g}) = 295$, $\nu_2(e_g) = 205$, and $\nu_5(t_{2g}) = 120$. (ν_1 is seen to be very close to our excited state value of 300.) It is clear that no prominent lines are attributable to the e_g or t_{2g} modes. Two weak features (lines α and β) appear about 100 and 130 cm^{-1}, respectively, from the no-phonon line and either may well correspond

to $\nu_5(t_{2g})$; another shoulder (line γ) about 194 cm^{-1} from the no-phonon line could reasonably be attributed to $\nu_2(e_g)$. Conceivably, one or more of these lines can also be assigned to the 16-cm^{-1} lattice progression (see bar spectrum, Fig. 2), though this seems unlikely for the 194-cm^{-1} shoulder. If ν_2 and/or ν_5 have been observed, they may gain their intensity through the Jahn-Teller mechanism. However, there is no evidence of the features expected for a strong Jahn-Teller effect[9,10,24]—strong progressions in the active modes with the appearance of a complex vibronic pattern. Aside from the obvious a_{1g} progression in ν_1, strong electron-lattice coupling is exhibited only in the low-frequency totally symmetric lattice modes previously discussed. No feature of the spectrum requires the Jahn-Teller effect for its explanation. The situation is similar to that in the U_u' Jahn-Teller susceptible state of $IrBr_6^{2-}$ (band 8),[4] where in fact the t_{2g} and e_g modes are very clearly seen without any indication of a strong Jahn-Teller effect.

Because e_g orbitals form σ bonds in octahedral complexes, states involving e_g electrons should be particularly Jahn-Teller susceptible.[24] It is therefore unfortunate that it has not been possible in this work to observe the higher-energy $E_u''(^2F_{5/2}) \rightarrow U_g'(^2E_g)$ transition which lies beyond 50 000 cm^{-1}.

The Jahn-Teller effect could also manifest itself through a Ham-effect quenching[24] of the spin-orbit coupling thus decreasing the separation of the $E_g''(^2T_{2g})$ and $U_g'(^2T_{2g})$ states from its expected value ($\sim \frac{3}{2}\zeta_d$). However, the magnitude of the observed decrease from the free-ion value is not at all unexpected,[19] and in view of the large energy separation, it seems extremely unlikely that a Ham effect is involved. Furthermore, a large Ham effect, such as the one which drastically quenches the spin-orbit coupling in the excited $^2T_{2u}$ charge-transfer manifold of $IrCl_6^{2-}$ also gives rise to a complex vibronic pattern.[3,25]

TABLE II. Assignment of vibrational structure in $Cs_2NaYCl_6:Ce^{3+}$.

Transition	Line	Energy (cm^{-1})	Assignment	ΔE[a] (cm^{-1})
$E_u''(^2F_{5/2}) \rightarrow U_g'(^2T_{2g})$	a	28 180	Hot band in $\nu(1)$[b]	−16[c]
	0	28 196	0 − 0	0
	b	28 210	$+\nu(1)$	14[c]
	c	28 228	$+2\nu(1)$	18
	$1l$	28 242	$+\nu(2)$[d]	46[c]
	d	28 260	$+4\nu(1)$	32[e]
	$2l$	28 288	$+2\nu(2)$	46
	α	28 296	$+\nu_5(t_{2g})$?[f]	100[c]
	β	28 326	$+\nu_5(t_{2g})$?[f]	130[c]
	$3l$	28 334	$+3\nu(2)$	46
	$4l$	28 380	$+4\nu(2)$	46
	γ	28 390	$+\nu_2(e_g)$?	196[c]
	$5l$	28 430	$+5\nu(2)$	50
	$6l$	28 478	$+6\nu(2)$	48
	1	28 502	$+\nu_1(a_{1g}): CeCl_6^{3-}$	306[c]
	2	28 798	$+2\nu_1(a_{1g})$	296
	3	29 096	$+3\nu_1(a_{1g})$	298
	4	29 398	$+4\nu_1(a_{1g})$	302
	5(?)	29 703	$+5\nu_1(a_{1g})$	305
$E_u''(^2F_{5/2}) \rightarrow E_g''(^2T_{2g})$	$0'$	29 435	0 − 0	0
	$1'l$	29 483	$+\nu(2)$[d]	48[c]
	$2'l$	29 533	$+2\nu(2)$	50
	$3'l$	29 573	$+3\nu(2)$	40
	$4'l$	29 618	$+4\nu(2)$	45
	$5'l$	29 668	$+5\nu(2)$	50
	$6'l$	29 708	$+6\nu(2)$	40
	$1'$	29 736	$+\nu_1(a_{1g}): CeCl_6^{3-}$	301[c]
	$2'$	30 038	$+2\nu_1(a_{1g})$	302
	$3'$	30 338	$+3\nu_1(a_{1g})$	300
	$4'$	30 633	$+4\nu_1(a_{1g})$	295
	$5'$	30 943	$+5\nu_1(a_{1g})$	310

[a]Energy from preceding line in progression unless noted otherwise.

[b]$\nu(1)$ is a ~16 -cm^{-1} a_{1g} lattice mode.

[c]Energy from appropriate 0-0 line.

[d]$\nu(2)$ is a ~45-cm^{-1} a_{1g} lattice mode. The frequencies corresponding to the progression in this mode are only listed for the first quantum of $\nu_1(a_{1g}): CeCl_6^{3-}$.

[e]$3\nu(1)$ would be unresolved from line $1l$ (see Fig. 2).

[f]Either line α or β could be ν_5 with the other a member of the $\nu(1)$ progression.

IV. CONCLUSIONS

The electric-dipole-allowed $4f^1 \rightarrow 5d^1$ transitions of octahedral Ce^{3+}, $E_u''(^2F_{5/2}) \rightarrow U_g'(^2T_{2g})$ and $E_u''(^2F_{5/2}) \rightarrow E_g''(^2T_{2g})$, have been identified using absorption and MCD techniques at liquid-helium temperature. The $U_g'(^2T_{2g})$ and $E_g''(^2T_{2g})$ excited states are split by ~1240 cm^{-1} due to spin-orbit coupling in the $5d$ orbital. The vibronic fine structure observed in both bands can be explained almost entirely in terms of progressions in $\nu_1(a_{1g})$ of the $CeCl_6^{3-}$ moiety with low-frequency lattice progressions superimposed. Most of the band intensity resides in the latter progressions. One quantum of the Jahn-Teller active modes $\nu_2(e_g)$ and/or $\nu_5(t_{2g})$ may appear as weak shoulders in the $U_g'(^2T_{2g})$ state, but there are no indications of a significant Jahn-Teller effect. $\Delta(\equiv 10Dq)$ is $\gtrsim$ 20 000 cm^{-1} in the excited state.

It is clear that Cs_2NaYCl_6 is an admirable host for optical studies. Ce^{3+} at high-dilution substitutes for Y^{3+} at precisely octahedral sites in the crystal, and there is every reason to expect that the same will be true for a variety of other ions. Thus optical studies should be possible on ions including lanthanides in the 3+ oxidation state at sites of octahedral symmetry.

ACKNOWLEDGMENTS

The authors are much indebted to Charles W. Magee for performing the high-resolution mass-spectrometric analysis on the crystal to determine Ce atom concentration. They have benefitted from several discussions with Dr. W. H. Inskeep. This work was supported by a grant from the National Science Foundation.

APPENDIX: CALCULATION OF MCD AND ABSORPTION PARAMETERS

For an isotropic molecule doped into a cubic host with longitudinal applied magnetic field, the MCD parameters A and C, and the dipole strength D, for the transition $a \rightarrow j$, can be expressed in molecule-fixed axes by[13]

$$A=\left(\frac{3}{2d_a}\right)\sum_{a\rightarrow j}(\langle j|\mu_z|j\rangle-\langle a|\mu_z|a\rangle)\times(|\langle a|m_+|j\rangle|^2-|\langle a|m_-|j\rangle|^2), \quad (1)$$

$$C=\left(\frac{3}{2d_a}\right)\sum_{a\rightarrow j}\langle a|\mu_z|a\rangle(|\langle a|m_+|j\rangle|^2-|\langle a|m_-|j\rangle|^2), \quad (2)$$

$$D=\left(\frac{3}{2d_a}\right)\sum_{a\rightarrow j}(|\langle a|m_+|j\rangle|^2+|\langle a|m_-|j\rangle|^2), \quad (3)$$

where d_a is the degeneracy of $|a\rangle$, $\vec{m}$ and $\vec{\mu}$ are, respectively, the electric and magnetic dipole operators, $m_+\equiv(-i/\sqrt{2})(m_x+im_y)$, $m_-\equiv(i/\sqrt{2})(m_x-im_y)$, and $|a\rangle$ and $|j\rangle$ are required to be diagonal in μ_z.

Using the basis functions, coupling tables, definitions, and conventions of Ref. 15, Eqs. (1)–(3) can be expressed in terms of reduced matrix elements for any specific transition.[26] For $E''\rightarrow U'$, the results are

$$A=-i[(3/2\sqrt{15})\langle U'||\mu||U'\rangle_1+(2/\sqrt{15})\times\langle U'||\mu||U'\rangle_2+(1/2\sqrt{3})\langle E''||\mu||E''\rangle]\times|\langle E''||m||U'\rangle|^2, \quad (4)$$

$$C=(i/2\sqrt{3})\langle E''||\mu||E''\rangle|\langle E''||m||U'\rangle|^2, \quad (5)$$

$$D=|\langle E''||m||U'\rangle|^2, \quad (6)$$

and for $E''_{(1)}\rightarrow E''_{(2)}$,

$$A=(i/\sqrt{3})(\langle E''_{(2)}||\mu||E''_{(2)}\rangle+\langle E''_{(1)}||\mu||E''_{(1)}\rangle)\times|\langle E''_{(1)}||m||E''_{(2)}\rangle|^2, \quad (7)$$

$$C=(-i/\sqrt{3})\langle E''_{(1)}||\mu||E''_{(1)}\rangle|\langle E''_{(1)}||m||E''_{(2)}\rangle|^2, \quad (8)$$

$$D=|\langle E''_{(1)}||m||E''_{(2)}\rangle|^2. \quad (9)$$

In these expressions, $\langle j||\mu||j\rangle$, $\langle a||m||j\rangle$, etc., are reduced matrix elements, $i=\sqrt{-1}$, and gerade and ungerade subscripts are usually omitted since whichever is applicable should be evident. $\langle U'|\mu_z|U'\rangle$ requires two independent reduced matrix elements (subscripts 1 and 2) because $T_1(\mu)\times U'$ contains U' twice.

It is necessary to evaluate the reduced matrix elements in Eqs. (4)–(9) to obtain the required results. This will be done in the present case by explicit use of relevant wave functions though the irreducible-tensor method as extended to the O^* double group by Dobosh[27] allows one to completely avoid the construction of wave functions in such problems. (The latter method is of great power in more complex problems and is well-suited for systematic tabulation and computerization.)

In the present case, the ground state is (approximately) $E''_u(^2F_{5/2})$. E'' for $J=\frac{5}{2}$ is explicitly tabulated in Griffith (Table A19[15]), and the $\frac{5}{2}$ functions can in turn be expressed in the L-S basis ($l=3$, $s=\frac{1}{2}$) using Clebsch-Gordon coefficients. The result for the α'' component is

$$|E''\alpha''\rangle=\frac{1}{\sqrt{7}}|3\,-\tfrac{1}{2}\rangle-\frac{1}{\sqrt{42}}|2\,\tfrac{1}{2}\rangle-\frac{\sqrt{10}}{\sqrt{42}}|-1\,-\tfrac{1}{2}\rangle+\frac{5}{\sqrt{42}}|-2\,\tfrac{1}{2}\rangle, \quad (10)$$

where the notation is $|m_l m_s\rangle$ for a $4f$ electron.

The $5d$ functions of the excited states, $U'_g(^2T_{2g})$ and $E''_g(^2T_{2g})$, can also be expressed in the L-S basis ($|m_l m_s\rangle$ for $l=2$, $s=\frac{1}{2}$) using Tables A20 and A24 of Griffith.[15] The results are

$$|E''\beta''\rangle=\frac{-\sqrt{2}}{\sqrt{3}}|1\,\tfrac{1}{2}\rangle-\frac{1}{\sqrt{6}}|2\,-\tfrac{1}{2}\rangle+\frac{1}{\sqrt{6}}|-2\,-\tfrac{1}{2}\rangle, \quad (11)$$

$$|U'\kappa\rangle=\frac{1}{\sqrt{3}}|1\,\tfrac{1}{2}\rangle-\frac{1}{\sqrt{3}}|2\,-\tfrac{1}{2}\rangle+\frac{1}{\sqrt{3}}|-2\,-\tfrac{1}{2}\rangle, \quad (12)$$

$$|U'\mu\rangle=|-1\,\tfrac{1}{2}\rangle. \quad (13)$$

Equations (10)–(13) give sufficient functions to evaluate all reduced matrix elements in Eqs. (4)–(9). To relate the dipole strengths (D) for the two transitions, both must be expressed in terms of a common element. This may be done using the well-known transition-dipole matrix elements for spherical harmonics.[28] The final results are, for $E''_u(^2F_{5/2})\rightarrow U'_g(^2T_{2g})$,

$$A/D=\tfrac{1}{42}(-35\kappa+50),\quad C/D=-\tfrac{5}{14},\quad D=\tfrac{500}{42}|\langle f||m||d\rangle|^2;$$

and for $E''_u(^2F_{5/2})\rightarrow E''_g(^2T_{2g})$,

$$A/D=-\tfrac{1}{21}(14\kappa+22),\quad C/D=\tfrac{5}{7},\quad D=\tfrac{10}{42}|\langle f||m||d\rangle|^2.$$

In these expressions, the ratios (A/D, C/D) are in units of Bohr magnetons, κ is the excited-state orbital reduction factor,[15] and $\langle f||m||d\rangle$ is a $4f\rightarrow 5d$ reduced-transition-dipole matrix element.

---

*Present address: Department of Chemistry, Louisiana State University, Baton Rouge, La. 70803.

[1]W. H. Inskeep, R. W. Schwartz, and P. N. Schatz, Mol. Phys. **25**, 805 (1973).
[2]S. B. Piepho, J. R. Dickinson, J. A. Spencer, and P. N. Schatz, Mol. Phys. **24**, 609 (1972).
[3]S. B. Piepho, J. R. Dickinson, J. A. Spencer, and P. N. Schatz, J. Chem. Phys. **57**, 982 (1972).
[4]J. R. Dickinson, S. B. Piepho, J. A. Spencer, and P. N. Schatz, J. Chem. Phys. **56**, 2668 (1972).

[5]See, for example, H. Weakliem, Phys. Rev. B **6**, 2743 (1972); T. C. Ensign and N. E. Byers, Phys. Rev. B **7**, 907 (1973); A. Kiel and W. B. Mims, Phys. Rev. B **6**, 34 (1972); R. W. Mires, D. I. Arnold, and W. K. Dean, Phys. Rev. B **5**, 3654 (1972); Y. Eisenberger and P. S. Pershan, Phys. Rev. **167**, 292 (1968).

[6]For earlier work on six-coordinate hexahalides, see J. L. Ryan and C. K. Jørgensen, J. Phys. Chem. **70**, 2845 (1966).

[7]L. R. Morss, M. Siegal, L. Stenger, and N. Edelstein, Inorg. Chem. **9**, 1771 (1970).

[8]D. G. Karraker, J. Chem. Phys. **55**, 1084 (1971).

[9]C. W. Struck and F. Herzfeld, J. Chem. Phys. **44**, 464 (1966).

[10]M. D. Sturge and M. H. Crozier, J. Chem. Phys. **46**, 4551 (1967).

[11]R. W. Schwartz and N. J. Hill, J. C. S. Faraday 2 (to be published).

[12]For general disucssions, see (a) D. S. McClure, *Electronic Spectra of Molecules and Ions in Crystals*, Part II (Academic New York, 1959); (b) C. K. Jørgensen, *Absorption Spectra and Chemical Bonding in Complexes* (Pergamon, London, 1962), Chap. 10.

[13]The MCD results are discussed using Serber's *A*, *B*, and *C* notation. The terms arise, respectively, from the Zeeman splitting of the transition, field-induced mixing of unperturbed states, and population differences within a Zeeman-split ground state. The *A* term dispersion is sigmoid with a zero at the absorption maximum, whereas *B* and *C* terms have their maximum (or minimum) there. For further discussion of these terms and for definitions, sign conventions, and units, see P. N. Schatz, A. J. McCaffery, W. Suëtaka, G. N. Henning, A. B. Ritchie, and P. J. Stephens, J. Chem. Phys. **45**, 722 (1966); P. N. Schatz and A. J. McCaffery, Q. Rev. Chem. Soc. **23**, 552 (1969); Q. Rev. Chem. Soc. **24**, 324 (E) (1970); A. D. Buckingham and P. J. Stephens, Annu. Rev. Phys. Chem. **17**, 399 (1966).

[14]R. A. Buchanan, H. E. Rast, and H. H. Caspers, J. Chem. Phys. **44**, 4063 (1966).

[15]J. S. Griffith, *The Theory of Transition-Metal Ions* (Cambridge U. P. Cambridge, England, 1964).

[16]J. C. Eisenstein and M. H. L. Pryce, Proc. R. Soc. A **255**, 181 (1960).

[17]A. Abragam and B. Bleaney, *Electron Paramagnetic Resonance of Transition Ions* (Oxford U. P. Oxford, England, 1970), p. 326.

[18]B. G. Wybourne, *Spectroscopic Properties of Rare Earths* (Interscience, New York, 1965), p. 41, Table 2-2.

[19]See, for example, Ref. 15, pp. 190–191; Ref. 18, p. 192..

[20]D. S. McClure and Z. Kiss, J. Chem. Phys. **39**, 3251 (1963).

[21]K. K. Rebane, *Impurity Spectra of Solids*, translated by J. S. Shier (Plenum, New York, 1970), Chap. 1.

[22]R. M. Hochstrasser and P. N. Prasad, J. Chem. Phys. **56**, 2814 (1972).

[23]John R. Ferraro, *Low-Frequency Vibrations of Inorganic and Coordination Compounds* (Plenum, New York, 1971), Table 6–7.

[24]See for example, M. D. Sturge, in *Solid State Physics*, edited by F. Seitz, D. Turnbull, and H. Ehrenreich (Academic, New York, 1967), Vol. 20, p. 91ff.

[25]W. C. Yeakel and P. N. Schatz (unpublished).

[26]In unpublished work Dobosh has derived completely general expressions for *A*, *C*, and *D* for both allowed and forbidden (vibronic) transitions for the groups *O* and *O** in terms of his *W* coefficients and reduced matrix elements (Ref. 27).

[27]P. A. Dobosh, Phys. Rev. A **5**, 2376 (1972).

[28]See, for example, John C. Slater, *Quantum Theory of Atomic Structure* (McGraw-Hill, New York, 1960), Vol. II, p. 224.